Journal of Solid Mechanics Vol. 10, No. 1 (2018) pp. 216-231

Calculation of Natural Frequencies of Bi-Layered Rotating Functionally Graded Cylindrical Shells

I. Fakhari Golpayegani *

Department of Mechanical Engineering, Golpayegan University of Technology, Golpayegan, Iran

Received 14 January 2018; accepted 17 March 2018

ABSTRACT

In this paper, an exact analytical solution for free vibration of rotating bi-layered cylindrical shell composed of two independent functionally graded layers was presented. The thicknesses of the shell layers were assumed to be equal and constant. The material properties of the constituents of bi-layered FGM cylindrical shell were graded in the thickness direction of the layers of the shell according to a volume fraction power-law distribution. In order to derive the equations of motion, the Sanders' thin shell theory and Rayleigh-Ritz method were used. Also the results were extracted by considering Coriolis, centrifugal and initial hoop tension effects. Effects of rotating speed, geometrical parameters, and material distribution in the two functionally graded layers of the shell, circumferential and longitudinal wave number on the forward and backward natural frequencies were investigated. A comparison of the results was made with those available in the literature for the validity and accuracy of the present methodology.

Keywords: Functionally graded material (FGM) ; Free vibration; Natural frequency; Bi-layered FGM cylindrical shell.

1 INTRODUCTION

MANY applications of circular cylindrical shells are found in engineering and industry fields, such as civil engineering, mechanical engineering, and aerospace engineering. Prior to their applications, their dynamic features, such as vibration, buckling, and stability are theoretically analyzed. This helps to avoid the future risks for their practical uses. In recent years, the use of functionally targeted materials (FGM) in environments with high temperatures has been considered. In fact, these materials are composites made of metals and ceramics in which the thermal insulation capability and good toughness of ceramics and metals can be used at the same time. FGM materials are inhomogeneous such that their properties change continuously and gradually from one level to another level. This operation can be applied by changing the volume ratio with a special equation. In recent years, research has been carried out on the field of free vibration of FGM cylindrical shells. Loy et al. [1] studied the spectra of the natural frequencies of functionally graded cylindrical shells for various geometrical parameters. They concluded that the influence of the material distribution was controlled by the volume fraction law. Najafizadeh and Isvandzibaei [2] studied the vibration of functionally graded shells based on the higher-order shear deformation plate theory with ring support. Arshad et al. [3] presented a frequency analysis of FGM cylindrical shells with various volume fraction laws. Shah et al. [4] also used exponential volume fraction law to study the vibration frequencies of FGM cylindrical

*Corresponding author. Tel.: +98 3157241566.
E-mail address: fakhari@gut.ac.ir (I. Fakhari Golpayegani)

shells by varying the base element of this law. Isvandzibaei and Awasare [5] analyzed the vibration of two kinds of functionally graded cylindrical shells with various volume fraction laws. Rahimi et al. [6] studied the vibrational behavior of functionally graded cylindrical shells with intermediate ring supports. A functionally graded cylindrical shell made up of a mixture of ceramic and metal was considered. The influence of some commonly used boundary conditions and the effect of changes in shell geometrical parameters and variations in ring support position on vibration characteristics was also studied. Studies on functionally graded (FG) cylindrical shell confined to a single layer can be seen in other literatures. Moradi-Dastjerdi and Foroutan [7] used different Mesh-Free method for free vibration analysis of orthotropic FGM cylinders. The cylinders are assumed to be a mixture of two isotropic materials as fiber and matrix. The volume fraction of the fiber is changed in the radial direction. Ebrahimi and Najafizadeh [8] analyzed the free vibration of a two-dimensional functionally graded circular cylindrical shell. The spatial derivatives of the equations of motion and boundary conditions were discretized by the methods of generalized differential quadrature (GDQ) and generalized integral quadrature (GIQ). Bahadori and Najafizadeh [9] investigated the dynamic behavior of moderately thick functionally graded cylindrical shell based on the First-order Shear Deformation Theory (FSDT). The material properties of functionally graded cylindrical shell were graded in two directional (radial and axial) and assumed to obey the power law distribution.

Two-layered FG cylindrical shells have many applications, such as nuclear reactors. Sofiyev et al. [10] analyzed the vibration and stability analysis of a three-layered conical shell with middle layer of functionally graded material. They applied the method of Galerkin to transform governing equations of motion into a pair of time dependent partial differential equations and came to a conclusion that the critical parameters were affected by the configurations of the constituent materials and the variation of the shell geometry. Arshad et al. [11] analyzed the vibration frequency of a bi-layered cylindrical shell composed of two independent functionally graded layers. The two thin layers were assumed to be perfectly bonded in the transverse direction at their interface without slip and their deformation was continuous across the layers interface. Arshad et al. [12] studied the vibration of bi-layered cylindrical shells with layers of different materials. One layer was made of functionally graded material and the other layer of isotropic material. Frequencies were evaluated for long, short, thick and thin cylindrical shells by varying the non-dimensional geometrical parameters, length-to-radius and thickness-to-radius ratios for a simply supported boundary condition. According to Shah et al. [13] the vibration characteristics of a cylindrical shell composed of three layers were investigated. The inner and outer layers of a cylindrical shell are functionally graded materials while the middle layer is of isotropic material. The wave propagation technique was used to solve the present shell problem. Sepiani et al. [14] investigated the free vibration and buckling of a two-layered cylindrical shell made of inner functionally graded (FG) and outer isotropic elastic layer, subjected to combined static and periodic axial forces. Li et al. [15] studied the free vibrations of a simply supported triple layer circular cylindrical shell with similar inner and outer isotropic layers and FGM core.

There exist a few studies on the rotating FGM cylindrical shells. One of these works was done by Ahmad and Naeem [16]. This paper utilized thin shell theory with Love approximation displacements field. As an effect of the rotation, only the centrifugal force was considered. Also, as an important part of the analysis, wave propagation technique was used and the vibration behavior of cylinder was approximated numerically by some beam Eigen functions. Civalek [17] using the discrete singular convolution (DSC) method, studied the free vibration analysis of rotating truncated conical shells, circular shells and panels. Isotropic, orthotropic, functionally graded materials (FGM) and laminated material cases were considered. Hosseini Hashemi et al. [18] presented an exact analytical solution for free vibration of a rotating functionally graded circular cylindrical shell based on Sanders' shear deformation theory. Effects of various combinations of boundary conditions, rotational speed, geometrical and material properties of the shell on the forward and backward waves of the natural frequencies were investigated. Mehrparar [19] analyzed vibration of functionally graded spinning cylindrical shells using higher order shear deformation theory.

According to advantageous literature review and based on the author's acknowledge, the absence of an exact analytical study is sensed for vibration analysis of a rotating multi-layered or bi-layered FGM cylindrical shells under Coriolis and centrifugal effects of axial rotation. In this paper, free vibration analysis of a rotating bi-layered cylinder made of functionally graded materials was considered. The equations of motion were obtained based on Sanders' shear deformation theory. Rotation was applied to the model by considering Coriolis, centrifugal and initial hoop tension effects. In order to derive the equations of the theory of thin shells, Rayleigh- Ritz method was applied. To make simply supported conditions, the components of displacement (in longitudinal direction, circumferential and radial) were considered as a combination of sine and cosine functions. The effect of various parameters, such as rotating speed, circumferential wave number, longitudinal wave number, and material distribution in the two functionally graded layers, thickness and length to radius ratios on natural backwards and forwards frequencies of rotating FGM cylindrical shells were also discussed. A number of comparisons with literature was done to check the effectiveness, robustness and accuracy of the presented method.

2 FUNCTIONALLY GRADED MATERIALS

FGM materials are made from a combination of two or more materials. Most of these materials are used in high temperature environments and the properties of these materials are defined as a function of temperature according to the following equation [1]:

$$P = P_0\left(P_{-1}T^{-1} + 1 + P_1T + P_2T^2 + P_3T^3\right) \tag{1}$$

where P_0, P_{-1}, P_1, P_2 and P_3 are constants at temperature T in Kelvin scale and are fixed for any specific matter. The characteristics of FGM, P related to ingredient properties and volume ratio and defined as follows [1]:

$$P = \sum_{j=1}^{k} P_j V_{fi} \tag{2}$$

P_j & V_{fi} in the aforementioned equation are the characteristics of materials and volume fraction *j*. Total volume ratio of materials is equal to one [1].

$$\sum_{j=1}^{k} \mathrm{V}_{fi} = 1 \tag{3}$$

For a cylindrical shell with a uniform thickness h and a reference surface at its middle surface, the volume fraction of the two constituents for a shell having a single FGM layer [1] can be expressed as:

$$V_1 = \left(\frac{2z+h}{2h}\right)^N \qquad V_2 = 1 - \left(\frac{2z+h}{2h}\right)^N \tag{4}$$

where N is the power law $(0 < N \le \infty)$ and z is the distance from middle surface $(-h/2 < z < +h/2)$.

For a bi-layered functionally graded cylindrical shell with the constituent materials M_1 and M_2 for inner FGM Layer, M_2 and M_3 for outer FGM layer, the effective material parameters Young's modulus *E*, Poisson's ratio *v* and the mass density *ρ* of both layers are expressed as [12]:

$$\begin{aligned}
E_{fgm}{}^1 &= (E_2 - E_1)[(2z+h)/h]^N + E_1 & E_{fgm}{}^2 &= (E_3 - E_2)[(2z+h)/h]^N + E_2 \\
\upsilon_{fgm}{}^1 &= (\upsilon_2 - \upsilon_1)[(2z+h)/h]^N + \upsilon_1 & \upsilon_{fgm}{}^2 &= (\upsilon_3 - \upsilon_2)[(2z+h)/h]^N + \upsilon_2 \\
\rho_{fgm}{}^1 &= (\rho_2 - \rho_1)[(2z+h)/h]^N + \rho_1 & \rho_{fgm}{}^2 &= (\rho_3 - \rho_2)[(2z+h)/h]^N + \rho_2
\end{aligned} \tag{5}$$

where $E_{fgm}{}^1, \upsilon_{fgm}{}^1, \rho_{fgm}{}^1$ and $E_{fgm}{}^2, \upsilon_{fgm}{}^2, \rho_{fgm}{}^2$ correspond to the resultant material properties for inner and outer FGM layers, respectively.

Fig. 1 shows that material M_1 is enriched at the inner surface of the inner layer and is gradually reduced in the thickness direction till it has zero concentration at the outer surface of the inner layer, while material M_2 is enriched at the outer surface of the inner layer and has zero concentration at the inner surface of the inner layer. Similarly, in the second layer material M_2 is concentrated at the inner surface of the outer layer and has zero concentration at the outer surface of the outer layer, while material M_3 is enriched at the outer surface of the outer layer and has zero concentration at the inner surface of the outer layer of the cylindrical shell. The material properties given in Eqs. (5) are for inner and outer FGM layers of the cylindrical shell which vary from $-h/2$ to 0 and from 0 to $+h/2$, respectively. From these relations, it can be concluded that at $z = -h/2$, the effective material properties become $E = E_1, \nu = \nu_1, \rho = \rho_1$ for inner layer, for $z = 0$, material properties become $E = E_2, \nu = \nu_2, \rho = \rho_2$ in both layers, and at $z = +h/2$, the material properties turn into $E = E_3, \nu = \nu_3$, and $\rho = \rho_3$ for functionally graded outer layer of the cylindrical shell. These results lead to the conclusion that there exists a smooth and continuous change in the material properties from material M_1 at the inner surface to the material properties of M_2 at the outer surface of the shell of the FGM inner layer of the cylindrical shell. Similarly in the outer layer, there is a variation in the material properties from material properties M_2 at the inner surface of the outer layer to material properties M_3 at the outer surface of the outer layer of the cylindrical shell. Similar behavior is seen in the inverse direction. For this shell, if the thickness to radius ratio is less than 0.05, it will be possible to use the theory of thin shells. In the next section, a formulation based on Sanders' shell theory, for a functionally graded cylindrical shell is carried out.

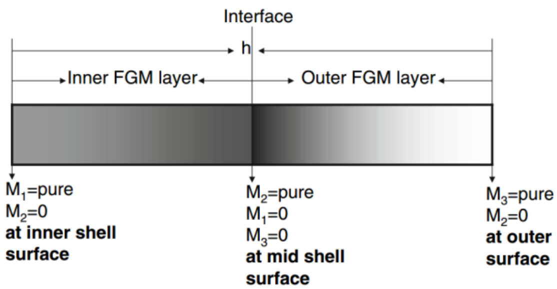

Fig.1
Variation of material properties along the thickness direction of the bi-layered FGM cylindrical shell [9].

3 THEORY AND EQUATIONS

The main purpose of this section is to obtain the equations of motion for FGM thin cylindrical shell shown in Fig. 2, with uniform thickness *h*, radius *R*, length *L* and mass density ρ, which rotates about the *x*-axis at constant angular velocity Ω. The shell has a coordinate system fixed on its middle surface. Membrane displacement in the longitudinal, circumferential and radial direction (x, θ, z) are shown by *u, v* and *w* and velocity vectors and displacements of a point on the shell are shown by $\bar{V}$ and $\bar{r}$, respectively. The velocity vector at each point of the shell is determined by the following equation.

$$\bar{V} = \dot{\bar{r}}(\Omega = 0) + (\Omega\bar{i} \times \bar{r}) \tag{6}$$

In this equation, the displacement vector $\bar{r}$ is written as:

$$\bar{r} = u\bar{i} + v\bar{j} + w\bar{k} \tag{7}$$

That $\bar{i}, \bar{j}$ and $\bar{k}$ are unit vectors in x and θ and z directions, respectively when $\Omega = 0$. By combining Eq. (7) with Eq. (6), the velocity vector is obtained as follows:

$$\bar{V} = \dot{u}\bar{i} + \dot{v}\bar{j} + \dot{w}\bar{k} + (\Omega\bar{i} \times w\bar{k}) + (\Omega\bar{i} \times v\bar{j}) \tag{8}$$

In this equation $\dot{u}, \dot{v}$ and $\dot{w}$ are velocity components in three main directions. The kinetic energy of the shell is expressed by following equation [20]:

$$T = \frac{1}{2} h \int_0^l \int_0^{2\pi} \rho_t \bar{V}\bar{V} R \; d\theta dx \tag{9}$$

By putting Eq. (8) into Eq. (9), the kinetic energy of the shell can be obtained as follows:

$$T = \frac{1}{2} h \int_0^L \int_0^{2\pi} \rho_t \left[\dot{u}^2 + \dot{v}^2 + \dot{w}^2 + 2\Omega\left(v\dot{w} - w\dot{v}\right) + \Omega^2 \left(v^2 + w^2\right) \right] R d\theta dx \tag{10}$$

where ρ_t is the mass density per unit length and is defined by:

$$\rho_t = \int_{-H/2}^{0} \rho^{fgm\,1} dz + \int_{0}^{H/2} \rho^{fgm\,2} dz \tag{11}$$

where $\rho^{fgm\,1}$ and $\rho^{fgm\,2}$ represent the mass density of the constituent materials in both the FGM layers.

The initial hope tension due to the centrifugal force is defined as [15]:

$$N_\theta = \rho h \Omega^2 R^2 \tag{12}$$

The strain energy of the shell due to hoop tension is given as [15]:

$$U_h = \frac{1}{2} \int_0^L \int_0^{2\pi} N_\theta \left\{ \left(\frac{1}{R} \frac{\partial u}{\partial \theta} \right)^2 + \left[\frac{1}{R} \left(\frac{\partial v}{\partial \theta} + w \right) \right]^2 + \left[\frac{1}{R} \left(\frac{\partial w}{\partial \theta} - v \right) \right]^2 \right\} R d\theta dx \tag{13}$$

Shell tensile and flexural strain energy can be written as follows [15]:

$$U_\varepsilon = \frac{1}{2} \int_0^L \int_0^{2\pi} \varepsilon^T \left[S \right] \varepsilon \ R \ d\theta dx \tag{14}$$

In this equation S is the stiffness matrix, and strain vector ε can be written as:

$$\varepsilon^T = \left\{ e_1 e_2 \ \gamma \ k_1 k_2 \ 2\tau \right\} \tag{15}$$

In this equation, the middle surface strain is determined by e_1, e_2, γ and the middle surface curvature is determined by k_1, k_2 and τ . Based on Sanders' thin shells theory, these values are calculated as follows. [21]

$$\begin{aligned}
e_1 &= \partial u / \partial x \\
e_2 &= (1/R)(w + \partial v / \partial \theta) \\
\gamma &= \partial v / \partial x + (1/R)\left(\partial u / \partial \theta\right) \\
k_1 &= -(\partial^2 w)/(\partial x^2) \\
k_2 &= -(1/R^2)((\partial^2 w)/(\partial \theta^2) + \partial v / \partial \theta) \\
\tau &= -\left(1/R\right)(\partial^2 w)/\partial x \partial \theta + \left(3/4R\right)\left(\partial v / \partial x\right) - \left(1/4R^2\right) \partial u / \partial \theta
\end{aligned} \tag{16}$$

Stiffness matrix for shell is given by:

$$\left[S \right] = \begin{bmatrix} A_{11} & A_{12} & 0 & B_{11} & B_{12} & 0 \\ A_{12} & A_{22} & 0 & B_{12} & B_{22} & 0 \\ 0 & 0 & A_{66} & 0 & 0 & B_{66} \\ B_{11} & B_{12} & 0 & D_{11} & D_{12} & 0 \\ B_{12} & B_{22} & 0 & D_{12} & D_{22} & 0 \\ 0 & 0 & B_{66} & 0 & 0 & D_{66} \end{bmatrix} \tag{17}$$

Here A_{ij} , B_{ij} and D_{ij} (*i, j* =1, 2 and 6) are extensional, coupling and bending stiffness's for isotropic materials, respectively and can be defined in both layers of the cylindrical shells as:

$$\left(A_{ij},B_{ij},D_{ij}\right)=\int_{-h/2}^{0}Q_{ij}^{fgm\,1}\left(1,Z,Z^2\right)dz+\int_{0}^{h/2}Q_{ij}^{fgm\,2}\left(1,Z,Z^2\right)dz \tag{18}$$

Reduced stiffness matrix Q determines by (18):

$$\begin{aligned}&Q_{11}=Q_{22}=\frac{E}{1-\upsilon^2}\\&Q_{12}=\frac{\upsilon E}{1-\upsilon^2}\\&Q_{66}=\frac{E}{2\left(1+\upsilon\right)}\end{aligned} \tag{19}$$

For a cylindrical shell with a simply-supported edge, the essential geometrical boundary at that edge conditions can be explicitly written as:

$$v=w=0 \tag{20}$$

Displacement functions *u, v* and *w* considered as follow:

$$\begin{aligned}&u=A_{mn}\cos\left(\lambda \mathrm{x}\right)\cos\left(n\theta+\omega t\right)\\&v=B_{mn}\sin\left(\lambda \mathrm{x}\right)\sin\left(n\theta+\omega t\right)\\&w=C_{mn}\sin\left(\lambda \mathrm{x}\right)\cos\left(n\theta+\omega t\right)\\&\lambda=m\pi/L\end{aligned} \tag{21}$$

A_{mn}, B_{mn} and C_{mn} are constant modes of shape coefficient, *m* is the number of half – wave longitudinal wave and *n* is the number of half –wave circumferential waves. By substituting Eq. (18) and (19) into (17), the stiffness matrix of the shell is calculated and by substituting Eq. (21) in Sanders' strain equations, the strain vector is calculated, and then according to Eq. (14), the potential energy of the shell can be obtained. The total energy of the system is given as follows:

$$\Pi=T-U_h-U_\varepsilon \tag{22}$$

Using the Ritz minimizing method,

$$\frac{\partial\Pi}{\partial\Delta}=0\qquad \Delta=A_{mn}\,,\;B_{mn}\,,\;C_{mn} \tag{23}$$

The following matrix relation is extracted:

$$\begin{bmatrix}\alpha_{11}&\alpha_{12}&\alpha_{13}\\\alpha_{21}&\alpha_{22}&\alpha_{23}\\\alpha_{31}&\alpha_{32}&\alpha_{33}\end{bmatrix}\begin{bmatrix}A\\B\\C\end{bmatrix}=\begin{bmatrix}0\\0\\0\end{bmatrix} \tag{24}$$

That α_{ij} presented at Appendix A. For obtaining a non-trivial answer of the aforementioned equations, the determinant matrix must be zero.

$$\begin{vmatrix} \alpha_{11} & \alpha_{12} & \alpha_{13} \\ \alpha_{21} & \alpha_{22} & \alpha_{23} \\ \alpha_{31} & \alpha_{32} & \alpha_{33} \end{vmatrix} = 0 \tag{25}$$

After expanding Eq. (25), the characteristic equations of membrane frequencies can be obtained as follows:

$$\beta_1\omega_{mn}^6 + \beta_2\omega_{mn}^4 + \beta_3\omega_{mn}^3 + \beta_4\omega_{mn}^2 + \beta_5\omega_{mn} + \beta_6 = 0 \tag{26}$$

That β_i are the constants. Maple toolbox is used to solve six roots of Eq. (26) for each *m* and *n*.

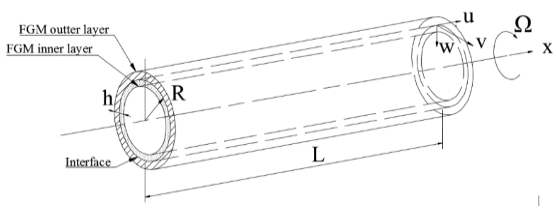

Fig.2
Rotating bi-layered FGM Cylindrical shell.

4 MATERIALS

Material properties used in this study is expressed in Table 1.

Table 1
Material properties of FGM.

material	$E(N\,m^{-2})\times 10^{11}$	ν	$\rho(kg\,m^{-3})\times 10^3$
Stainless steel (*SS*)	2.07788	0.317756	8.166
Zirconia (*Zr*)	1.6806296	0.297996	5.7
Nickel (*Ni*)	2.05098	0.31	8.9
Alumina (Al_2O_3)	3.8	0.3	3.8
Aluminum (*Al*)	0.7	0.34	2.7

5 RESULTS AND DISCUSSIONS

5.1 Validation

The validation and the accuracy of the present approach were checked by comparing the present results and those found in other research work. In Table 2., the results of the variation of natural frequencies of the five types of bi-layered functionally graded cylindrical shells with circumferential wave number *n*=1,2,3,4,5 having shell parameters *(m=1, L/R=20, h/R=0.002)* and material parameters at power law exponent *N*=5 were compared with the results of Arshad et al. [12].

Table 2
Comparison of natural frequencies (*Hz*) with circumferential wave number *n* for power law exponent *N* =5 with geometrical parameters *(m=1, h/R=0.002, L/R=20)* for simply supported bi-layer FGM cylindrical shells.

Material	*Ni-Zr-SS*		*Ni-SS-Zr*		*SS-Ni-Zr*		*SS-Zr-Ni*		*Zr-Ni-SS*	
n	Arshad [12]	Present	Arshad [12]	Present	Arshad [12]	Present	Arshad [12]	Present	Arshad [12]	Present
1	13.645	13.6453	13.322	13.3218	13.266	13.2655	13.915	13.9149	13.512	13.5119
2	4.6257	4.6222	4.5108	4.5110	4.4853	4.4852	4.7113	4.7070	4.5808	4.5827
3	4.3313	4.3185	4.1502	4.1509	4.1284	4.1281	4.4087	4.3923	4.2154	4.2234
4	7.3665	7.3509	7.0123	7.0130	6.9889	6.9886	7.5069	7.4870	7.1114	7.1213
5	11.775	11.7587	11.198	11.1988	11.168	11.1673	12.005	11.9838	11.35	11.3608
Average error = 0.08 %										

Table 3. shows the natural frequencies of FG cylinder under different rotational speeds (from 0 to 200 *rev/s*). The natural frequencies were calculated for a FGM cylinder with material properties of $Al\text{-}AL_2O_3$ and mode numbers m=n=1. From the table, the columns for each rotation speed are considered, which show the forward (F_f) and backward wave (F_b) frequencies, respectively. The forward waves correspond to the decreasing frequencies and the backward ones corresponded to the increasing frequencies. It can be concluded from this table that there is a very good agreement between the present method and the reference results [18] for any rotation speeds. This is evident from the average errors calculated between the present method and reference results which are written in Table 3.

Table 3
Comparison of natural frequency for a rotating single layer FGM cylinder (*h/R=0.01, L/R=3, N=1, n=m=1*, *AL*-Alumina).

Ω (*rad/s*)	F_f (*Hz*)		F_b (*Hz*)	
	Hosseini [18]	Present	Hosseini [18]	Present
0	518	516.979	518	516.979
25	493.8	492.829	542.13	541.116
50	469.56	468.664	566.2	565.237
100	420.91	420.293	614.16	613.434
150	372.07	371.871	661.85	661.567
200	323.04	323.398	709.22	709.633
Average error = 0.16 %				

By confirming the accuracy of the present method for FGM rotating single layer shell and FGM bi-layered Cylindrical shell, free vibration of rotating bi-layered FGM cylindrical shell is considered in the model for the next step.

Table 4. shows the natural frequencies of rotating bi-layered (*Ni+ Alumina +SS*) FGM cylindrical shell and single-layered (*Ni+SS*) rotating FGM cylindrical shells under different rotational speeds (from 100 to 300 *rev/s*). The natural frequencies are calculated for circumferential wave number n=1, 2, 3, 4, 5 with axial half-wave number m=1 for non-dimensional geometrical parameters L/R=6, h/R=0.002 and the power law index N=1.

Table 4
Variation of natural frequency for a rotating FGM cylinder (*h/R=0.002, L/R=6, N=1, m=1*).

Material		*Ni - SS*		*Ni - Alumina - SS*	
Ω (*rad/s*)	*n*	F_f (*Hz*)	F_b (*Hz*)	F_f (*Hz*)	F_b (*Hz*)
100	1	100.1401991	130.4571539	146.5772404	176.8890497
	2	35.77269753	61.22057579	52.63012126	78.06903425
	3	34.56792159	53.74863081	39.63836802	58.81210419
	4	50.49271596	65.53155008	52.12428596	67.15752278
	5	68.63007905	80.91283158	69.65166867	81.92973837
200	1	84.96719304	145.6014162	131.4110797	192.0348618
	2	33.24044088	84.15932636	47.80308912	98.69277564
	3	60.25946048	98.66417214	63.21518305	101.5848221
	4	98.14657459	128.2703164	99.02184604	129.1118986
	5	135.2184504	159.827155	135.7668476	160.3450902
300	1	69.7843282	160.7364481	116.2379858	207.1740678
	2	34.34705423	110.7828983	46.60145883	122.9655595
	3	87.66271463	145.3775427	89.77785992	147.3876114
	4	146.317858	191.6183111	146.9891929	192.1831291
	5	202.1602929	239.1811246	202.6050621	239.5276255

As mentioned, the frequencies of the cylinder depend on the rotational speed and rotation direction. Indeed, rotation in the positive direction presents a decreasing behavior in the natural frequencies and rotation in the negative direction presents an increasing behavior in the natural frequencies. Hence, the natural frequencies of rotating cylinder versus rotational speed bifurcate into two branches as the forward and backward whirl, respectively. Constituent materials used for the fabrication of single-layered FGM cylindrical shells have the same configuration as the constituents at the inner and outer FGM layers of the bi-layered FGM cylindrical shells. It is observed that natural frequencies of the bi-layered FGM cylindrical shells are above the frequencies of single-layered FGM cylindrical shells for different rotational speeds. Therefore, the addition of an intermediate layer is seen as being evident in the improved vibration characteristics of the shell.

5.2 Effect of rotation on the various mode numbers

The variation of natural frequencies of a FGM cylinder with properties as *L/R=6* and *h/R=0.002* is plotted under rotational speed according to Fig. 3(a-c), for various longitudinal (*n*) and circumferential mode (*m*) numbers. The rotational speed changes between 0 and 200 *rev/s*. From the figure, it can be observed that there is a decrease in the difference of the frequency between backward and forward with increasing circumferential wave number *n*, while this difference increases with increasing rotating speed Ω. At small circumferential wave number (*n*), the frequency of the backward wave increases and that of forward wave decreases with increasing rotating speed Ω. With large value of *n*, the frequency of both backward and forward wave increases with increasing rotating speed Ω. By increasing the longitudinal wave number (*m*), the backward and forward frequencies are increased. Based on these figures, it can be said that there exist a substantial influence of rotating speed Ω and circumferential wave number n on the frequency characteristics. When rotating speed Ω is large and circumferential wave number *n* is small, these influences become more significant. It is observed that the forward and backward frequencies according to the first longitudinal wave $n = m = 1$ show more changes by increasing the rotational speed with respect to the other mode numbers.

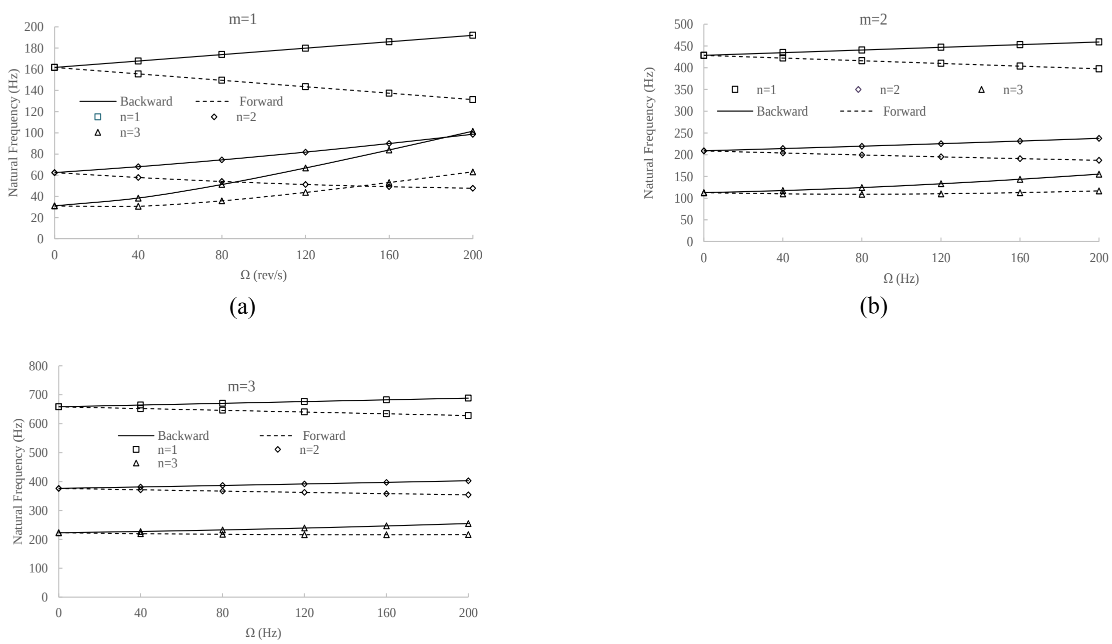

(a) (b) (c)

Fig.3
Variation of natural frequencies of a bi-layered FGM cylindrical shell versus rotational speed for various mode numbers (*Ni-Alumina-SS*, *L/R*=6,*h/R*=0.002, *N*=1, 1<*m*<3, 1<*n*<3).

5.3 Variation of natural frequencies with circumferential wave number n for different material type

In Table 5., the results of the variation of natural frequencies of the eight types of bi-layered functionally graded cylindrical shells with circumferential wave number *n*=1,2,3,4,5 *m*=1 having shell parameters (*L/R*=6,*h/R*=0.002, *N*=1) for two rotation speed are presented. It can be seen from these tables that the backward and forward natural frequencies (*Hz*) of the bi-layered functionally graded cylindrical shell are directly and indirectly affected by the variation of rotation speed, respectively. The material type have a great impact on the backward and forward frequency, so that the highest frequency occurs in *Al - Alumina - Zr* FGM shell and the lowest frequency occurs *Alumina - Zr - Ni* FGM shell. Increasing the rotational speed reduces the environmental wave number (*n*) of fundamental natural frequencies, but material type change does not affect it. It was also observed that in the high environmental wave number (*n*), there is a reduction in the effect of the material type on the natural backward and forward frequencies between all material types.

Table 5
Variation of natural frequency for a rotating FGM cylinder (*h/R=0.002, L/R=6, N=1, m=1*).

Ω (*rev/s*)	*n*	F_f (*Hz*)	F_b (*Hz*)	F_f (*Hz*)	F_b (*Hz*)	F_f (*Hz*)	F_b (*Hz*)	F_f (*Hz*)	F_b (*Hz*)
		Ni - Alumina - SS		*SS- Alumina -Ni*		*Ni-Zr- Alumina*		*Alumina -Zr-Ni*	
100	1	146.57724	176.88905	146.57661	176.88841	129.92425	160.23285	129.88575	160.19387
	2	52.63012	78.06903	52.62288	78.06158	46.48278	71.92321	46.49393	71.92269
	3	39.63837	58.81210	39.62574	58.79892	37.70032	56.88780	37.74335	56.90018
	4	52.12429	67.15752	52.11320	67.14552	51.57148	66.62901	51.63469	66.64249
	5	69.65167	81.92974	69.64304	81.91987	69.46053	81.77232	69.54057	81.78432
300	1	116.23799	207.17407	116.23735	207.17343	99.58516	190.51177	99.54716	190.47233
	2	46.60146	122.96556	46.59632	122.95977	41.94578	118.32609	41.97814	118.32364
	3	89.77786	147.38761	89.77407	147.38214	88.92946	146.60217	89.02593	146.60702
	4	146.98919	192.18313	146.98770	192.17891	146.70812	191.99804	146.86159	192.00273
	5	202.60506	239.52763	202.60540	239.52424	202.42830	239.47372	202.63614	239.47782
		Ni - Alumina - Al		*Al - Alumina - Ni*		*Al - Alumina - SS*		*Al - Alumina - Zr*	
100	1	157.04819	187.35933	157.07972	187.39119	160.67347	190.98628	170.14879	200.45824
	2	56.50788	81.94174	56.50378	81.94568	57.84981	83.29359	61.35361	86.79154
	3	40.90829	60.07039	40.88301	60.06628	41.34733	60.53160	42.53971	61.71850
	4	52.49075	67.50572	52.45033	67.49963	52.61641	67.66645	53.00450	68.04822
	5	69.77801	82.03143	69.72520	82.02559	69.83735	82.13844	70.05784	82.35130
300	1	126.71132	217.64531	126.74251	217.67748	130.33540	221.27438	139.81550	230.74435
	2	49.63966	125.98308	49.62060	125.98808	50.68345	127.05479	53.50493	129.85492
	3	90.35062	147.91516	90.28570	147.91357	90.48383	148.11146	91.01884	148.62285
	4	147.17767	192.30586	147.07274	192.30372	147.13304	192.36274	147.29522	192.49834
	5	202.72419	239.56250	202.58146	239.56050	202.62134	239.59925	202.72462	239.67248

5.4 Variation of natural frequencies with circumferential wave number (n), rotation speed and power law exponent

In Table 6., the variations of the natural frequencies (*Hz*) are tabulated with the circumferential wave numbers (*n*) at *m*=1 having geometrical parameters, *L/R*=20, *h/R*=0.002 for the four rotation speed of bi-layered functionally graded cylindrical shells with simply supported end conditions at power law exponents *N*=0.01,1,4,7. It can be seen from these table that there is a decrease in the forward and backward natural frequencies (*Hz*) of the bi-layered functionally graded cylindrical shell with increasing power law exponent *N*. Also by increasing the circumferential wave number (*n*) for each rotation speed, forward and backward frequencies decreased. Another result of this table is that the effect of power law exponent at large *n* and Ω are small on forward and backward natural frequencies.

In Fig. 4, the variations of the natural frequencies (*Hz*) are shown with the rotation speed Ω at *n*=1 having geometrical parameters, *L/R*=6, *h/R*=0.002 for the three longitudinal wave number *m*=1, 5, 10 at power law exponents *N*=0.01, 1, 7. It can be seen from these figures that the forward and backward natural frequencies (*Hz*) of the bi-layered functionally graded cylindrical shell are indirectly affected by the variation of power law exponent *N*. Also it can be observed that the influence of power law exponent *N* at large longitudinal wave number m is more significant than that at small longitude nal wave number *m*.

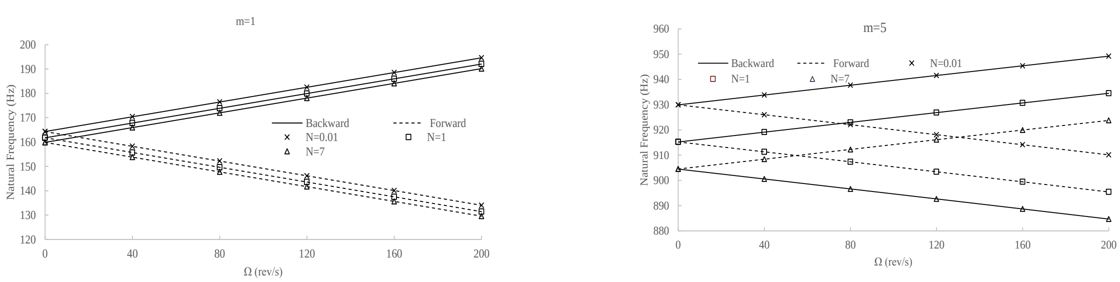

(a) (b)

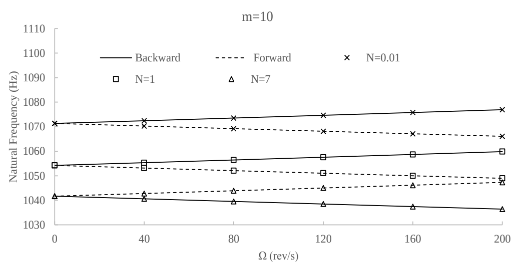

(c)

Fig.4
Variation of natural frequencies of a bi-layered FGM cylindrical shell versus rotational speed for various power law index (*Ni-Alumina -SS, L/R=6,h/R=0.002, n=1*).

Table 6
Variation of natural frequency for a rotating FGM cylinder (*h/R=0.002, L/R=6, N=1, m=1*).

		N=0.01		*N*=1		*N*=4		*N*=7	
Ω (*rev/s*)	*n*	F_f (*Hz*)	F_b (*Hz*)	F_f (*Hz*)	F_b (*Hz*)	F_f (*Hz*)	F_b (*Hz*)	F_f (*Hz*)	F_b (*Hz*)
0	1	164.3109	164.3109	161.7365	161.7365	160.2329	160.2329	159.8642	159.8642
	2	63.5073	63.5073	62.4942	62.4942	61.8983	61.8983	61.7521	61.7521
	3	31.6596	31.6596	31.0969	31.0969	30.7871	30.7871	30.7175	30.7175
	4	20.6891	20.6891	20.1184	20.1184	19.9078	19.9078	19.8955	19.8955
	5	19.6415	19.6415	18.7359	18.7359	18.5511	18.5511	18.6169	18.6169
100	1	149.1517	179.4633	146.5772	176.8890	145.0740	175.3850	144.7054	175.0161
	2	53.6039	79.0362	52.6301	78.0690	52.0588	77.5004	51.9187	77.3609
	3	40.0113	59.1675	39.6384	58.8121	39.4343	58.6181	39.3884	58.5747
	4	52.3468	67.3516	52.1243	67.1575	52.0370	67.0873	52.0287	67.0833
	5	69.9188	82.1580	69.6517	81.9297	69.5829	81.8846	69.5933	81.9009
200	1	133.9859	194.6092	131.4111	192.0349	129.9082	190.5303	129.5397	190.1613
	2	48.6797	99.5558	47.8031	98.6928	47.2910	98.1864	47.1657	98.0623
	3	63.4636	101.7975	63.2152	101.5848	63.0789	101.4692	63.0480	101.4433
	4	99.1810	129.2135	99.0218	129.1119	98.9505	129.0752	98.9398	129.0731
	5	135.9623	160.4620	135.7668	160.3451	135.6961	160.3220	135.6925	160.3303
300	1	118.8131	209.7486	116.2380	207.1741	114.7353	205.6690	114.3670	205.2998
	2	47.3687	123.7116	46.6015	122.9656	46.1555	122.5288	46.0466	122.4219
	3	89.9810	147.5354	89.7779	147.3876	89.6655	147.3073	89.6397	147.2894
	4	147.1457	192.2514	146.9892	192.1831	146.9114	192.1585	146.8968	192.1571
	5	202.8027	239.6060	202.6051	239.5276	202.5170	239.5122	202.5045	239.5177

5.5 Variation of natural frequencies (Hz) with non-dimensional geometrical parameters (L/R, h/R, h/L)

Fig. 5 shows the variation of the fundamental natural frequency with the *L/R* ratio. The fundamental frequencies of the backward and forward wave for the rotating cylindrical shell decrease rapidly with *L/R* ratio, and then the values become nearly constant. The effect of rotating speed for the large *L/R* ratio is greater than that for the small *L/R* ratio.

In Table 7., the variations of the fundamental natural frequencies (*Hz*) are tabulated with the *L/R* at *m*=1 having geometrical parameters, *h/R*=0.002 for the two rotation speed of bi-layered functionally graded cylindrical shells with simply supported end conditions at power law exponents *N*=0.01, 1, 7. The effects of *N* on fundamental natural forward and backward frequencies for each rotation speed in high *L/R* ratio are less than small *L/R* ratio. The column n^* represent the circumferential wave numbers at which the fundamental frequencies occur. It is noted that with increase in *L/R* ratio and rotation speed the n^* decreased.

Table 7
Variation of fundamental natural frequencies of a bi-layered FGM cylindrical shell versus *L/R* (*Ni- Alumina -SS*, *h/R=0.002*).

N		0.01		1		7		n^*
Ω (*rev/s*)	*L/R*	F_f (*Hz*)	F_b (*Hz*)	F_f (*Hz*)	F_b (*Hz*)	F_f (*Hz*)	F_b (*Hz*)	
50	1	143.7876	146.9473	140.3610	143.5645	139.3485	142.5849	10
	5	35.7969	43.3073	35.3380	42.8626	35.1053	42.6404	4
	10	18.0728	27.6283	17.8958	27.4600	17.8137	27.3844	3
	15	8.1732	20.9004	8.0243	20.7548	7.9246	20.6574	2
200	1	276.3176	294.2837	273.9078	291.9921	272.3549	290.5252	7
	5	69.2223	107.6031	68.8080	107.2245	68.5198	106.9614	3
	10	19.6668	70.5799	19.4458	70.3725	19.2885	70.2244	2
	15	1.3920	63.9303	0.8800	63.4184	0.5046	63.0429	1

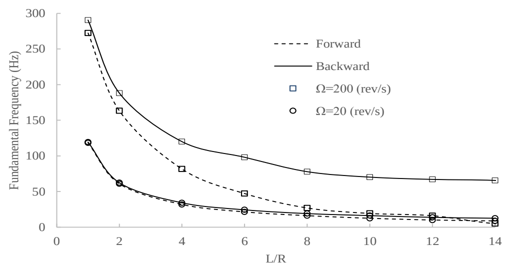

Fig.5
Variation of fundamental natural frequencies of a bi-layered FGM cylindrical shell versus *L/R* (*Ni- Alumina -SS*, *h/R=0.002, N=7*).

The variation of natural frequencies of a FGM cylinder with properties as *L/R*=1, 2, 3 and *h/R*=0.002 is plotted under rotational speed according to Fig. 6, for various longitudinal (*m*) and circumferential mode (*n*) numbers. The rotational speed changes between 0 and 200 *rev/s*. The forward and backward frequencies according to *n*=1 and *m*=1 show more changes by increasing the rotational speed with respect to the other mode numbers. It can be seen from these figures that the forward and backward natural frequencies (*Hz*) of the bi-layered functionally graded cylindrical shell decrease with increasing *L/R* ratio.

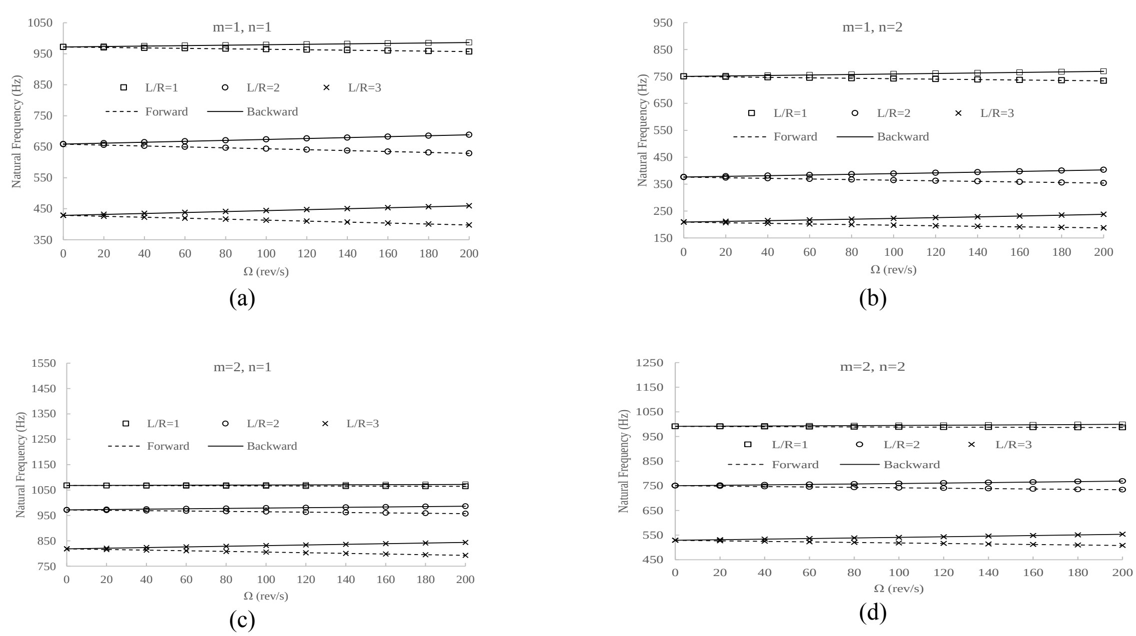

Fig.6
Variation of natural frequencies of a FG cylinder versus rotational speed for various mode numbers (*Ni- Alumina -SS*, *L/R*=1, 2, 3, *h/R*=0.002, *N*=1, $1\leq m\leq 2$; $1\leq n\leq 2$).

Fig. 7 shows the variation of the fundamental frequency with the *h/R* ratio. There is an increase in the fundamental frequencies of the backward and forward wave of the cylindrical shell with increase in *h/R* ratio at any rotating speed. The effect of rotating speed for the large *h/R* ratio is greater than that for the small *h/R* ratio.

In Table 8., the variations of the fundamental natural frequencies (*Hz*) are tabulated with the *h/R* at *m*=1 having geometrical parameters, *L/R*=1 for the two rotation speed of bi-layered functionally graded cylindrical shells with simply supported end conditions at power law exponents *N*=0.01, 1, 7. The effects of *N* on fundamental natural forward and backward frequencies for each rotation speed in high *h/R* ratio are greater than small *h/R* ratio. It is noted that with increasing *h/R* ratio and rotation speed the n^* decreased.

The variation of natural frequencies of a FG cylinder with properties as *h/R*=0.002, 0.02, 0.05 and *L/R*=1 is plotted under rotational speed in Fig. 8, for various longitudinal (*m*) and circumferential mode (*n*) numbers. The rotational speed changes between 0 and 200 *rev/s*. It is observed that the forward and backward frequencies according to *n*=2 and *m*=1 show more changes by increasing the rotational speed with respect to the other mode numbers. It can be seen from these figures that the forward and backward natural frequencies (*Hz*) of the bi-layered functionally graded cylindrical shell increase with increasing *h/R* ratio, and this effect for large *m* and *n* mode numbers is greater than for the small m and n mode numbers.

Table 8
Variation of fundamental natural frequencies of a bi-layered FGM cylindrical shell versus *h/R* (*Ni- Alumina -SS*, *L/R*=1).

N		0.01		1		7		n^*
Ω (*rev/s*)	*h/R*	F_f (*Hz*)	F_b (*Hz*)	F_f (*Hz*)	F_b (*Hz*)	F_f (*Hz*)	F_b (*Hz*)	
50	0.002	143.7876	146.9473	140.3610	143.5645	139.3485	142.5849	10
	0.01	267.1317	271.5061	256.4544	260.9759	254.3190	258.9516	7
	0.03	448.7643	454.5320	429.4836	435.5449	425.5841	431.8678	5
	0.05	570.5250	577.2898	547.0368	554.1646	541.6141	549.0180	4
200	0.002	276.3176	294.2837	273.9078	291.9921	272.3549	290.5252	7
	0.01	321.3305	341.6254	313.9685	334.7547	311.2858	332.4413	6
	0.03	462.1489	485.2495	443.1787	467.4535	439.0015	464.1662	5
	0.05	570.7997	597.8911	547.0668	575.6094	541.2278	570.8749	4

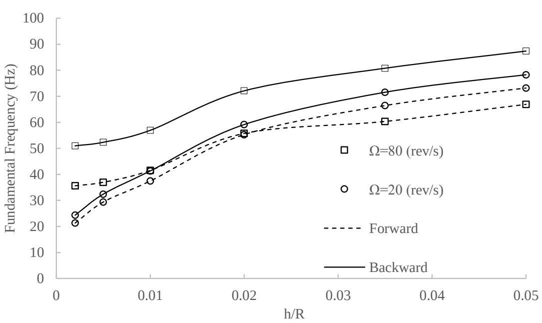

Fig.7
Variation of fundamental natural frequencies of a bi-layered FGM cylindrical shell versus *h/R* (*Ni- Alumina -SS*, *L/R=6, N=7*).

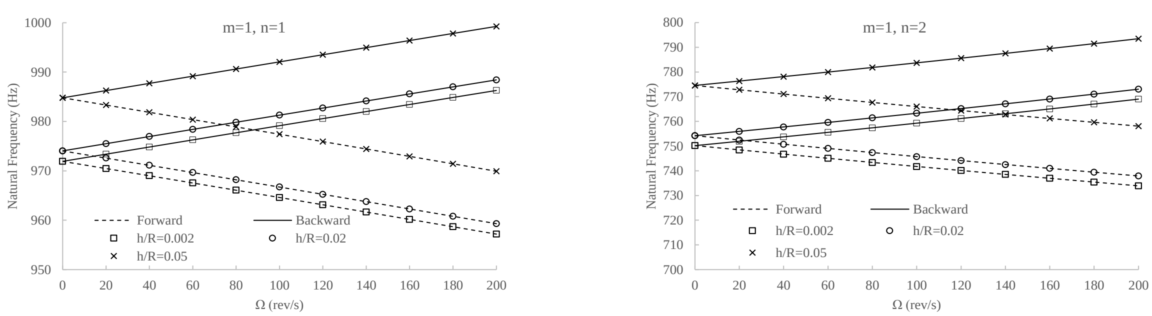

(a) (b)

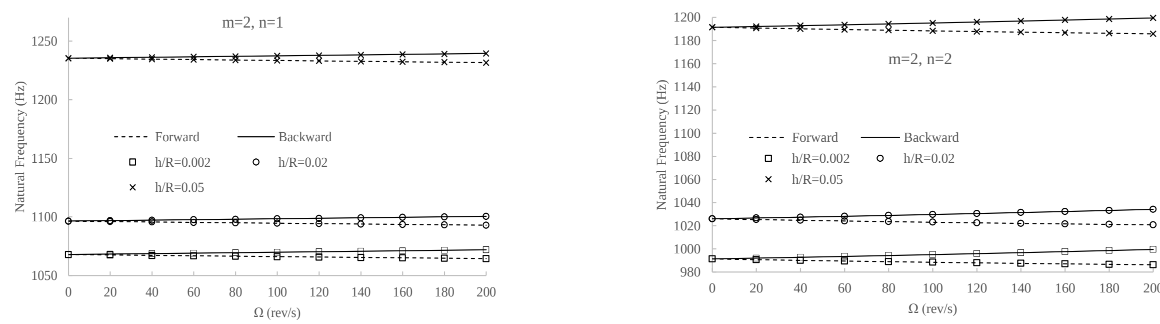

(c) (d)

Fig.8
Variation of natural frequencies of a FG cylinder versus rotational speed for various mode numbers (*Ni- Alumina -SS*, *L/R*=1, *h/R*=0.002, 0.02, 0.05, *N*=1, $1\leq m\leq 2$; $1\leq n\leq 2$).

The variation of natural frequencies of a FGM cylinder with properties as *R/L*=0.25, 0.5 and *h/L*=0.002, 0.02, 0.05 are plotted under rotational speed according to Fig. 9, for *m*=*m*=1. The forward and backward frequencies according to *R/L*=0.5 show more changes by increasing the rotational speed with respect to the *R/L*=0.25. It can be seen from these figures that the forward and backward natural frequencies (*Hz*) of the bi-layered functionally graded cylindrical shell increase with increasing *h/L* ratio.

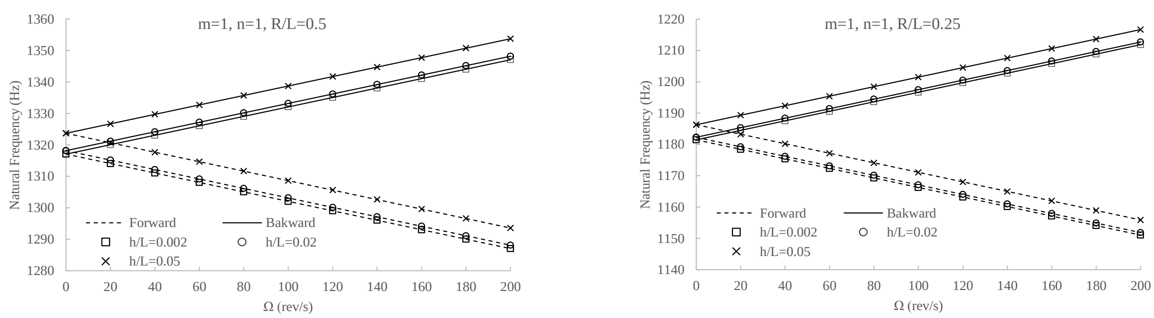

(a) (b)

Fig.9
Variation of natural frequencies of a FG cylinder versus rotational speed for *h/L*(*Ni- Alumina -SS*, *R/L*=0.25, 0.5, *h/L*=0.002, 0.02, 0.05, *N*=1).

6 CONCLUSIONS

By using the Sanders' shell theory, the vibration analysis for the rotating FGM bi-layered cylindrical shell was investigated. The natural frequencies were compared with the previously published results for the rotating FGM single layer shell and the bi-layered non rotating cylindrical shells. It was observed that the proposed exact method yielded accurate results in comparison with the references. The backward wave frequencies were higher than the forward frequencies due to Coriolis effects. The higher the rotating speed the larger the gap generated between the backward and forward waves frequencies at any vibration mode. The addition of an intermediate layer helped to improve the vibration characteristics of the shell. The material type had great impact on the backward and forward frequency. It can be seen that the forward and backward natural frequencies (*Hz*) of the bi-layered functionally graded cylindrical shell decreased by increasing the power law exponent *N*. Moreover, a change in the power law exponent had no effect on the circumferential wave number *n* at which the fundamental frequencies of the shells occurred. The fundamental frequencies of the backward and forward wave for the rotating cylindrical shell decreased rapidly with *L/R* ratio at high rotating speed, and then the values became nearly constant. The effect of rotating speed for the large *L/R* ratio was greater than for the small *L/R* ratio. It can be seen that the forward and backward natural frequencies (*Hz*) of the bi-layered functionally graded cylindrical shell increased with increasing *h/R* and *h/L* ratios and this effect for large *m* and *n* mode numbers was greater than for the small *m* and *n* mode numbers, also . The fundamental frequencies of the backward and forward wave for the rotating cylindrical shell increased with *h/R* ratio.

ACKNOWLEDGMENTS

Research reported in this paper was supported by Golpayegan University of Technology under award number 94500/3141-March 5, 2016.

APPENDIX A

$$\alpha_{11}=\left(\frac{\pi}{8LR(1-\nu_{fgm1}^2)(1-\nu_{fgm2}^2)}\right)(4\rho_t R^2L^2\omega^2\nu_{fgm1}^2+4\rho_t R^2L^2\omega^2\nu_{fgm2}^2-hL^2n^2E_{fgm2}\nu_{fgm1}^2-hL^2n^2E_{fgm1}\nu_{fgm2}^2-hL^2n^2E_{fgm2}\nu_{fgm2}$$
$$-hL^2n^2E_{fgm1}\nu_{fgm1}+hL^2n^2E_{fgm1}+hL^2n^2E_{fgm2}-2hm^2\pi^2R^2E_{fgm2}\nu_{fgm1}^2-2hm^2\pi^2R^2E_{fgm1}\nu_{fgm2}^2+4R^2\rho_t L^2n^2\Omega^2$$
$$+4R^2\Omega^2\rho_t L^2n^2\nu_{fgm2}^2\nu_{fgm1}^2+2hm^2\pi^2R^2E_{fgm1}+2hm^2\pi^2R^2E_{fgm2}-4\rho_t R^2L^2\omega^2\nu_{fgm2}^2\nu_{fgm1}^2+hL^2n^2E_{fgm2}\nu_{fgm1}^2\nu_{fgm2}$$
$$+hL^2n^2E_{fgm1}\nu_{fgm1}\nu_{fgm2}^2-4\rho_t R^2L^2\omega^2-4R^2\Omega^2\rho_t L^2n^2\nu_{fgm1}^2-4R^2\Omega^2\rho_t L^2n^2\nu_{fgm2}^2)$$

$$\alpha_{12}=\left(\frac{\pi^2hmn}{16R(1-\nu_{fgm1}^2)(1-\nu_{fgm2}^2)}\right)(hE_{fgm1}\nu_{fgm2}^2-hE_{fgm2}\nu_{fgm1}^2+2RE_{fgm1}+2RE_{fgm2}-2RE_{fgm2}\nu_{fgm1}^2-2RE_{fgm1}\nu_{fgm2}^2+2RE_{fgm1}\nu_{fgm1}$$
$$+2RE_{fgm2}\nu_{fgm2}-2RE_{fgm2}\nu_{fgm2}\nu_{fgm1}^2-2RE_{fgm1}\nu_{fgm1}\nu_{fgm2}^2+hE_{fgm2}-hE_{fgm1})$$

$$\alpha_{13}=\left(\frac{\pi^2hm}{16RL^2(1-\nu_{fgm1}^2)(1-\nu_{fgm2}^2)}\right)(-hm^2\pi^2R^2E_{fgm1}+hm^2\pi^2R^2E_{fgm2}+hL^2n^2E_{fgm1}\nu_{fgm2}^2-hL^2n^2E_{fgm2}\nu_{fgm1}^2+4L^2RE_{fgm1}\nu_{fgm1}$$
$$+4L^2RE_{fgm2}\nu_{fgm2}-4L^2RE_{fgm1}\nu_{fgm1}\nu_{fgm2}^2-4L^2RE_{fgm2}\nu_{fgm2}\nu_{fgm1}^2+hL^2n^2E_{fgm2}-hL^2n^2E_{fgm1}+hm^2\pi^2R^2E_{fgm1}\nu_{fgm2}^2)$$

$$\alpha_{21}=\alpha_{12}$$

$$\alpha_{22}=\left(\frac{\pi}{48RL^3(1-\nu_{fgm1}^2)(1-\nu_{fgm2}^2)}\right)(24\rho_t R^4L^2\omega^2\nu_{fgm2}^2\nu_{fgm1}^2+12hL^2R^2n^2E_{fgm1}\nu_{fgm2}^2+12hL^2R^2n^2E_{fgm2}\nu_{fgm1}^2$$
$$-24R^4\Omega^2\rho_t L^2n^2\nu_{fgm2}^2\nu_{fgm1}^2+n^2h^3L^2E_{fgm2}\nu_{fgm1}^2+6L^2Rn^2h^2E_{fgm1}-6L^2Rn^2h^2E_{fgm2}-12hL^2R^2n^2E_{fgm1}$$
$$-12hL^2R^2n^2E_{fgm2}-24R^4\Omega^2\rho_t L^2n^2-24\rho_t R^4L^2\omega^2\nu_{fgm1}^2-24\rho_t R^4L^2\omega^2\nu_{fgm2}^2+24R^4\Omega^2\rho_t L^2n^2\nu_{fgm1}^2$$
$$+24\rho_t R^4L^2\omega^2-n^2h^3L^2E_{fgm1}-n^2h^3L^2E_{fgm2}-6L^2Rn^2h^2E_{fgm1}\nu_{fgm2}^2+6L^2Rn^2h^2E_{fgm2}\nu_{fgm1}^2+n^2h^3L^2E_{fgm1}\nu_{fgm2}^2$$
$$+24R^4\Omega^2\rho_t L^2n^2\nu_{fgm2}^2-6hR^4m^2\pi^2E_{fgm2}-6hR^4m^2\pi^2E_{fgm1}-2m^2\pi^2h^3R^2E_{fgm1}-2m^2\pi^2h^3R^2E_{fgm2}$$
$$+6R^3m^2\pi^2h^2E_{fgm1}-6R^3m^2\pi^2h^2E_{fgm2}-2h^3\pi^2R^2m^2E_{fgm2}\nu_{fgm1}^2\nu_{fgm2}-6h^2\pi^2R^3m^2E_{fgm2}\nu_{fgm1}^2\nu_{fgm2}$$
$$-2h^3\pi^2R^2m^2E_{fgm1}\nu_{fgm1}\nu_{fgm2}^2+6h^2\pi^2R^3m^2E_{fgm1}\nu_{fgm1}\nu_{fgm2}^2-6h\pi^2R^4m^2E_{fgm2}\nu_{fgm1}^2\nu_{fgm2}$$
$$-6h\pi^2R^4m^2E_{fgm1}\nu_{fgm1}\nu_{fgm2}^2+2h^3\pi^2R^2m^2E_{fgm1}\nu_{fgm1}-6h^2\pi^2R^3m^2E_{fgm1}\nu_{fgm1}-6R^3m^2\pi^2h^2E_{fgm1}\nu_{fgm2}^2$$
$$+6R^3m^2\pi^2h^2E_{fgm2}\nu_{fgm1}^2+2m^2\pi^2h^3R^2E_{fgm2}\nu_{fgm1}^2+2m^2\pi^2h^3R^2E_{fgm1}\nu_{fgm2}^2+2h^3\pi^2R^2m^2E_{fgm2}\nu_{fgm2}$$
$$+6h^2\pi^2R^3m^2E_{fgm2}\nu_{fgm2}+6h\pi^2R^4m^2E_{fgm2}\nu_{fgm2}+6h\pi^2R^4m^2E_{fgm1}\nu_{fgm1}+6hR^4m^2\pi^2E_{fgm2}\nu_{fgm1}^2$$
$$+6hR^4m^2\pi^2E_{fgm1}\nu_{fgm2}^2)$$

$$\alpha_{23}=\left(\frac{\pi}{48RL^3(1-\nu_{fgm1}^2)(1-\nu_{fgm2}^2)}\right)(-48\rho_t R^4L^2\Omega\omega\nu_{fgm2}^2\nu_{fgm1}^2-48R^4\Omega^2\rho_t L^2n\nu_{fgm2}^2\nu_{fgm1}^2-48R^4\Omega^2\rho_t L^2n-48\rho_t R^4L^2\Omega\omega$$
$$+n^3h^3L^2E_{fgm1}\nu_{fgm2}^2+n^3h^3L^2E_{fgm2}\nu_{fgm1}^2+3L^2Rh^2nE_{fgm1}+3L^2Rn^3h^2E_{fgm1}-3L^2Rn^3h^2E_{fgm2}-3L^2Rh^2nE_{fgm2}-12hL^2R^2nE_{fgm1}$$
$$-12hL^2R^2nE_{fgm2}-n^3h^3L^2E_{fgm2}-n^3h^3L^2E_{fgm1}-3L^2Rh^2nE_{fgm1}\nu_{fgm2}^2+3L^2Rh^2nE_{fgm2}\nu_{fgm1}^2-3L^2Rn^3h^2E_{fgm1}\nu_{fgm2}^2$$
$$+48R^4\Omega^2\rho_t L^2n\nu_{fgm1}^2+48R^4\Omega^2\rho_t L^2n\nu_{fgm2}^2+48\rho_t R^4L^2\Omega\omega\nu_{fgm1}^2+48\rho_t R^4L^2\Omega\omega\nu_{fgm2}^2+12hL^2R^2nE_{fgm2}\nu_{fgm1}^2$$
$$+12hL^2R^2nE_{fgm1}\nu_{fgm2}^2+3L^2Rn^3h^2E_{fgm2}\nu_{fgm1}^2+2m^2\pi^2h^3R^2nE_{fgm1}\nu_{fgm2}^2-3R^3nh^2m^2\pi^2E_{fgm1}\nu_{fgm2}^2+m^2\pi^2h^3R^2\nu_{fgm1}E_{fgm1}$$
$$+m^2Pi^2h^3R^2\nu_{fgm2}E_{fgm2}+3R^3nh^2m^2\pi^2E_{fgm2}\nu_{fgm1}^2+2m^2\pi^2h^3R^2nE_{fgm2}\nu_{fgm1}^2-m^2\pi^2h^3R^2\nu_{fgm1}E_{fgm1}\nu_{fgm2}^2-m^2\pi^2h^3R^2\nu_{fgm2}E_{fgm2}\nu_{fgm1}^2$$
$$-2m^2Pi^2h^3R^2nE_{fgm2}+3R^3nh^2m^2\pi^2E_{fgm1}-3R^3nh^2m^2\pi^2E_{fgm2}-2m^2\pi^2h^3R^2nE_{fgm1})$$

$$\alpha_{31} = \alpha_{13}$$

$$\alpha_{32} = \alpha_{23}$$

$$\begin{aligned}
\alpha_{33} = &\left(\frac{\pi}{48R^3L^3(1-\nu_{fgm1}^2)(1-\nu_{fgm2}^2)}\right)(24\rho_t R^4L^4\omega^2 - n^4h^3L^4E_{fgm2} - n^4h^3L^4E_{fgm1} - 12hL^4R^2E_{fgm1} - 12hL^4R^2E_{fgm2} + 6L^4Rh^2n^2E_{fgm1} \\
&-24R^4\Omega^2\rho_t L^4n^2\nu_{fgm2}^2\nu_{fgm1}^2 + 6L^2R^3h^2m^2\pi^2\nu_{fgm1}E_{fgm1} - 6L^2R^3h^2m^2\pi^2\nu_{fgm2}E_{fgm2} - 2m^2\pi^2h^3R^2n^2L^2E_{fgm1} - 2m^2\pi^2h^3R^2n^2L^2E_{fgm2} \\
&-6L^2R^3h^2m^2\pi^2\nu_{fgm1}E_{fgm1}\nu_{fgm2}^2 + 6L^2R^3h^2m^2\pi^2\nu_{fgm2}E_{fgm2}\nu_{fgm1}^2 + 2m^2\pi^2h^3R^2n^2L^2E_{fgm1}\nu_{fgm2}^2 + 2m^2\pi^2h^3R^2n^2L^2E_{fgm2}\nu_{fgm1}^2 \\
&-m^4\pi^4h^3R^4E_{fgm2} - m^4\pi^4h^3R^4E_{fgm1} + m^4\pi^4h^3R^4E_{fgm1}\nu_{fgm2}^2 + m^4\pi^4h^3R^4E_{fgm2}\nu_{fgm1}^2 + 6L^4Rh^2n^2E_{fgm2}\nu_{fgm1}^2 - 6L^4Rh^2n^2E_{fgm1}\nu_{fgm2}^2 \\
&+24R^4\Omega^2\rho_t L^4n^2\nu_{fgm1}^2 + 24R^4\Omega^2 rhotL^4n^2\nu_{fgm2}^2 + 24rhotR^4L^4\omega^2\nu_{fgm2}^2\nu_{fgm1}^2 + n^4h^3L^4E_{fgm1}\nu_{fgm2}^2 + n^4H^3L^4E_{fgm2}\nu_{fgm1}^2 - 24R^4\Omega^2 rhotL^4n^2 \\
&-24\rho_t R^4L^4\omega^2\nu_{fgm1}^2 - 24\rho_t R^4L^4\omega^2\nu_{fgm2}^2 + 12hL^4R^2E_{fgm1}\nu_{fgm2}^2 + 12hL^4R^2E_{fgm2}\nu_{fgm1}^2 - 6L^4Rh^2n^2E_{fgm2})
\end{aligned}$$

REFERENCES

[1] Loy C. T., Lam K. Y., Reddy J. N., 1999, Vibration of functionally graded cylindrical shells. *International Journal of Mechanical Sciences* **41**: 309-324.

[2] Najafizadeh M. M., Isvandzibaei M. R., 2007, Vibration of functionally graded cylindrical shells based on higher order shear deformation plate theory with ring support, *Acta Mechanica* **191**: 75-91.

[3] Arshad S. H., Naeem M. N., Sultana N., 2007, Frequency analysis of functionally graded material cylindrical shells with various volume fraction laws, *Proceedings of the Institution of Mechanical Engineers, Part C: Journal of Mechanical Engineering Science* **221**: 1483-1495.

[4] Shah A. G., Mahmood T., Naeem M. N., 2009, Vibrations of FGM thin cylindrical shells with exponential volume fraction law, *Applied Mathematics and Mechanics* **30**: 607-615.

[5] Isvandzibaei M. R., Awasare P. J., 2009, Comparison of two kinds of functionally graded cylindrical shells with various volume fraction laws for vibration analysis, *Journal of Solid Mechanics* **1**: 190-200.

[6] Rahimi G. H., Ansari R., Hemmatnezhad M., 2011, Vibration of functionally graded cylindrical shells with ring support, *Scientia Iranica* **18**: 1313-1320.

[7] Moradi-Dastjerdi R., Foroutan M., 2014, Free vibration analysis of orthotropic FGM cylinders by a mesh-free method, *Journal of Solid Mechanics* **6**: 70-81.

[8] Ebrahimi M. J., Najafizadeh M. M., 2014, Free vibration analysis of two-dimensional functionally graded cylindrical shells, *Applied Mathematical Modelling* **38**: 308-324.

[9] Bahadori R., Najafizadeh M. M., 2015, Free vibration analysis of two-dimensional functionally graded axisymmetric cylindrical shell on Winkler–Pasternak elastic foundation by first-order shear deformation theory and using Navier-differential quadrature solution methods, *Applied Mathematical Modelling* **39**: 4877-4894.

[10] Sofiyev A. H., Deniz A., Akçay I. H., Yusufoğlu E., 2006, The vibration and stability of a three-layered conical shell containing an FGM layer subjected to axial compressive load, *Acta Mechanica* **183**: 129-144.

[11] Arshad S. H., Naeem M. N., Sultana N., Shah A. G., Iqbal Z., 2011, Vibration analysis of bi-layered FGM cylindrical shells, *Archive of Applied Mechanics* **81**: 319-343.

[12] Arshad S. H., Naeem M. N., Sultana N., Iqbal Z., Shah A. G., 2010, Vibration of bilayered cylindrical shells with layers of different materials, *Journal of Mechanical Science and Technology* **24**: 805-810.

[13] Shah A., Naeem M., Mahmood T., Arshad S., 2013, Vibration analysis of three-layered functionally graded cylindrical shells with isotropic middle layer resting on Winkler and Pasternak foundations, *Pakistan Journal of Science* **65**: 256-262.

[14] Sepiani H., Rastgoo A., Ebrahimi F., Arani A. G., 2010, Vibration and buckling analysis of two-layered functionally graded cylindrical shell, considering the effects of transverse shear and rotary inertia, *Materials & Design* **31**: 1063-1069.

[15] Li S.-R., Fu X.-H., Batra R. C., 2010, Free vibration of three-layer circular cylindrical shells with functionally graded middle layer, *Mechanics Research Communications* **37**: 577-580.

[16] Ahmad M., Naeem M., 2009, Vibration characteristics of rotating FGM circular cylindrical shells using wave propagation method, *European Journal of Scientific Research* **36**: 184-235.

[17] Civalek Ö., 2017, Discrete singular convolution method for the free vibration analysis of rotating shells with different material properties, *Composite Structures* **160**: 267-279.

[18] Hosseini-Hashemi S., Ilkhani M. R., Fadaee M., 2013, Accurate natural frequencies and critical speeds of a rotating functionally graded moderately thick cylindrical shell, *International Journal of Mechanical Sciences* **76**: 9-20.

[19] Mehrparvar M., 2009, Vibration analysis of functionally graded spinning cylindrical shells using higher order shear deformation theory, *Journal of Solid Mechanics* **1**: 159-170.

[20] Zhao X., Liew K., Ng T., 2002, Vibrations of rotating cross-ply laminated circular cylindrical shells with stringer and ring stiffeners, *International Journal of Solids and Structures* **39**: 529-545.

[21] Sanders Jr J. L., 1959, *An Improved First-Approximation Theory for Thin Shells*, NASA TR R-24, U.S.